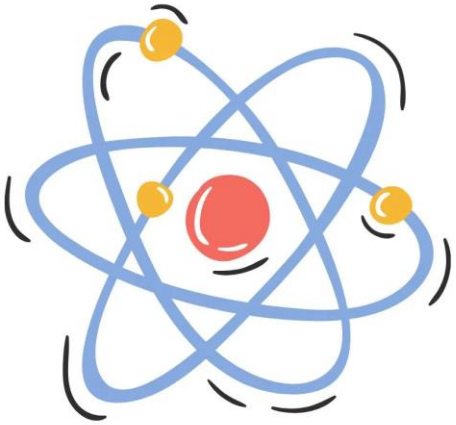

JOURNAL OF DYNAMICS AND CONTROL

VOLUME 9 ISSUE 1: 35 - 47

# DEVELOPMENT AND VALIDATION OF AN EFFICIENT NOISE POLLUTION ENERGY CONVERSION SYSTEM

**Arunesh Kumar Singh, Shahida Khatoon, Kriti Tripathi**

Department of Electrical Engineering, Jamia Millia Islamia, New Delhi-110025, India

DOI: https://doi.org/10.71058/jodac.v9i1005

# Development and Validation of an Efficient Noise Pollution Energy Conversion System

**Arunesh Kumar Singh[1], Shahida Khatoon[2], Kriti Tripathi[3]**

[1, 2, 3] *Department of Electrical Engineering, Jamia Millia Islamia, New Delhi-110025, India*

***[1]asingh1@jmi.ac.in, [2]skhatoon@jmi.ac.in, [3]tripathikriti@gmail.com***

***Abstract***— *Noise pollution is one of the repercussions of modernization. Noise pollution is an acoustic pressure signal that has the potential to produce low-level electrical signals and thus the main objective of the research work is to optimize the electrical signal produced from the noise pollution so that any unwanted sound can be referred to as Noise. With the advancement in technology, various compact and highly efficient sensors suitable for acoustic energy conversion are commercially available and these sensors can convert the sound pressure level (SPL) into a suitable low-level electric signal. A suitable amplification-rectification unit can improve the quality of the electrical signal and the power management unit must be used for the storage of the energy. This paper presents the development and validation of an effective and better experimental model for noise pollution energy conversion. The developed model is tested in a real environment under diverse conditions. The proposed model has produced a 1.72 V electrical signal at 101dB SPL input, without any amplification. The developed amplifier module is designed to support the low-level electrical signal and provides a voltage gain of $2\times10^3$. The application outcomes justify the superiority of this model over others as available in the literature.*

***Keywords***— *Acoustic energy, Electrical energy, Energy conversion, Noise pollution, SPL signal.*

## 1. INTRODUCTION

Sound energy is a readily available resource accessible to everyone. The invention of the telephone in 1876 marked a significant milestone in converting sound signals into electrical pulses. As time progressed, a wide range of microphones and loudspeakers emerged, all with the purpose of transmitting voices over long distances. During the mid-19th century, the carbon microphone was invented, allowing for the conversion of sound signals into electrical ones. Today, there are three commonly employed principles for converting acoustic energy into electrical energy: electrostatic, electromagnetic, and piezoelectric. Additionally, combinations of these conversion mechanisms are referred to as hybrid techniques, such as thermo-acoustic and triboelectric mechanisms. Sound itself is the result of mechanical energy released when an object vibrates, while the sound pressure level (SPL) serves as a measure of noise pollution. Figure 1 illustrates the various steps involved in the process of converting noise pollution energy. These small energy packets derived from noise pollution can prove valuable in energizing remotely located sensors within a Wireless Sensor Network (WSN).

This paper is divided into five sections: literature review, components of mathematical modeling, hardware modeling, and experimental setup & improvements, and result & analysis. In the next section, literature analysis of the various prototypes based on acoustoelectric transformation systems has been discussed.

DOI: https://doi.org/10.71058/jodac.v9i1005

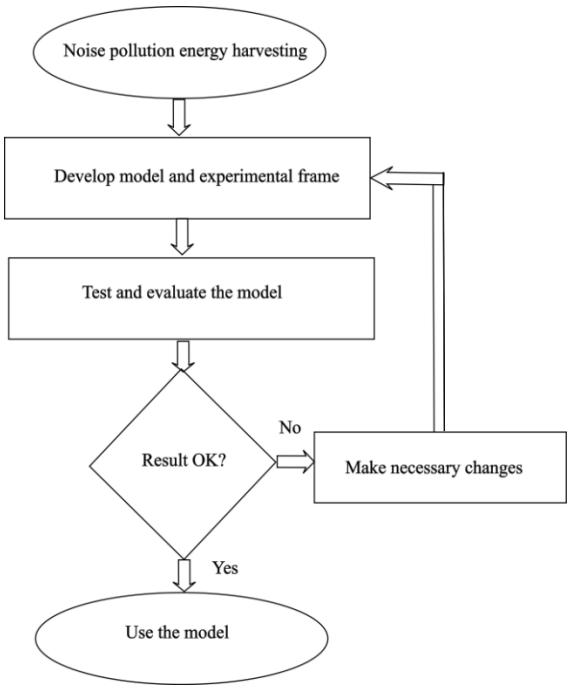


Fig. 1 Steps involved in noise pollution energy conversion.

## 2. LITERATURE REVIEW

A critical review of the various prototypes sound to electrical energy conversion system with model output and application is consolidated in Table 1.

TABLE I. Comparative review of various prototype sound-electric energy conversion systems.

| Model Name, Year & Reference No. | Input Type, Level | Output | Application |
|---|---|---|---|
| MEMS AEH, 2006, [1] | Sound, 149dB | 0.34μW/cm2 & up to 250 μW/cm2 | For Aero acoustic application |
| Self-powered electroacoustic liner system, 2008, [2] | Sound, Upto153 dB, 2.5kHz | Tuned resonance frequency, 212 Hz | Suppression of aircraft engine noise. |
| Lightening Rabbit, 2010,[3] | Sound, up to 130 dB | Voltage, 0.006V | Battery charging |
| Single & Dual mass VEH, 2012, [4] | Force | Power | Vehicle suspension, road irregularity |
| Noise Energy generating device, 2012, [5] | Frequency, 110 Hz-140Hz | 19.1 mV-16.8 mV & 0.614mW-0.47mW | Tunnels, Green Development Era |
| Low freq. AEH, 2013, [6] | Sound, 100 dB, 199 Hz frequency | 1.51V, 0.498 mW | Low-power generation |
| Sound to electric power conversion, 2013, [7] | Sound signal at 2kHz frequency | Voltage, 200mV | Battery charging |
| Multilayer PVDF in HR for EH, 2013, [8] | 15 Pa at 850Hz | 0.19 μW | Low-power generation |
| Hybrid AEH, 2016, [9] | 130dB-2.1kHz | 2.2 μW, up to 123mV | Self-powered WSN |

DOI: https://doi.org/10.71058/jodac.v9i1005

| | | | |
|---|---|---|---|
| Sound wave EH, 2017, [10] | 96 dB sound using speaker | 2.057mW | Low power devices, green energy |
| Traffic noise EH Standalone system, 2017, [11] | Sound, 75 dB average at 5.6 m distance | 0.78V/ hour, 0.0325W/ hour, | Capacitor Charging |
| Low frequency AEH using HR, 2017, [12] | 100 dB SPL | 3.49 µW | Low power devices |
| PVDF film with graphene and metal electrode, 2017, [13] | 105 dB, 1V at 155 Hz | 0.7 V | Capacitor Charging |
| AEH noise barrier for high-speed train, 2018, [14] | SPL, 110dB | 74.6mV & 1.24 | Low power electronic devices, Replaces conventional noise barrier |
| AEH using piezo, 2018, [15] | Sound, 100 dB, at 147Hz frequency | 0.7 V | Between car sections of High-Speed Train |
| Sonic energy conversion, 2019, [16] | SPL, above 70 dB | 0.024-watt/hour | Street lightning |
| EH system from noise, 2021, [17] | Sound, 75-114dB | 2-28mV | For high sound pollution area |
| Multi frequency sound energy harvesting, 2021, [18] | Sound, 100 dB | 5.31-8.66nW | Supply power for wake up a radio with 4.5nW power consumption |
| Triboelectric nano-generator, 2021, [19] | Sound, 90 dB, 140 Hz | 1.5 V, 58% efficiency. | Powering a sensor for continuous Humidity & Temperature monitoring |

Figure 2 provides a comparison of the output voltage with respect to the input SPL among the results of the cited papers.

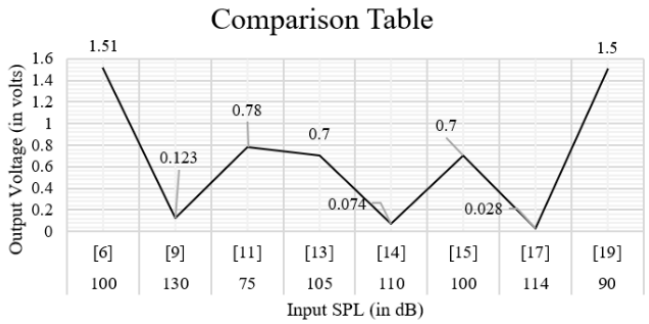


Fig. 2 Comparison graph of input SPL vs output voltage of cited papers.

## 3. MATHEMATICAL MODELING

### 3.1 Sound Propagation in Air

In the air, the sound propagates in longitudinal wave format (vibrates in the direction of propagation). The mathematical expression for the propagation of plane wave sound is given by,

$$\frac{d^2p}{dx^2} - \frac{1}{c^2}\frac{d^2p}{dt^2} = 0 \quad (1)$$

The relation between sound speed wavelength, and frequency is given by,

$$c=\lambda f \quad (2)$$

Here, speed of sound is represented as c, wavelength as λ, frequency of sound as f, and sound pressure as p respectively. The Leq (equivalent sound pressure level) is expressed in terms of sound pressure level as follows:

DOI: https://doi.org/10.71058/jodac.v9i1005

$$L_P = 20\log\left(\frac{\mathrm{p}}{p_{\mathrm{ref}}}\right) \quad (3)$$

Here, p is the sound pressure (in Pascal) of approximately 20 micro-Pascal.
The sound pressure level, Leq will decrease by six decibels for every doubling of the source-object distance.
The sound intensity of the sound source is given as follows:

$$S_I = \frac{p}{A} \quad (4)$$

Here, area is given by $A = 4\pi r^2$
According to Griffiths & Langdon's Model,

$$L_{eq} = L_{50} + \frac{(L_{10}-L_{90})^2}{56} \quad (5)$$

Here, the equivalent sound pressure levels L10, L50, and L90 respectively exceeded SPL levels of 10, 50, and 90 percentiles of duration (time-period) [20].

### 3.2 Loudspeaker

The loudspeaker acts as a sound source. The sound pressure is produced by the cone motion of the loudspeaker. The sinusoidal signal is applied to the loudspeaker. Consider a voltage signal applied to a loudspeaker is given by,

$$V(t) = V_0 \sin \omega t \quad (6)$$

The relation between voltage and cone's displacement 'x' depends upon various parameters of the loudspeaker motor such as voice coil, magnet, and suspension. The displacement of cone motion depends upon the loudspeaker motor. Consider a voltage that drives the cone with the magnitude $x_0$ given by,

$$x = x_0 \sin \omega t \quad (7)$$

Therefore, the velocity and acceleration of the cone are expressed as,

$$v = \frac{\mathrm{dx}}{\mathrm{dt}} = \omega \mathrm{x}_0 \cos \omega t \quad (8)$$

$$a = \frac{\mathrm{dv}}{\mathrm{dt}} = -\omega^2 x_0 \sin \omega t \quad (9)$$

The cone's pressure is expressed as,

$$p = \frac{\rho \mathrm{S}}{2\pi \mathrm{r}} a = -\frac{\rho \mathrm{S}}{2\pi \mathrm{r}} \omega^2 x = \frac{\rho \mathrm{S}}{2\pi \mathrm{r}} \frac{V_0 \mathrm{BL}}{R_{\mathrm{LM}} M_{\mathrm{LM}}} \sin \omega t \quad (10)$$

Here, $\rho$ is the density, $S$ is the cone's surface area, r is the cone's displacement, $M_{\mathrm{LM}}$ is the moving mass, $R_{\mathrm{LM}}$ is the DC resistance of a purely resistive loudspeaker, BL is the force factor.
The current is the amount of charge that flows per second.

$$I = \frac{\mathrm{dQ}}{\mathrm{dt}} \quad (11)$$

The immobile electric charge is generated between the two electrodes of the piezo sensor, forming a capacitor C.

$$V = \frac{1}{C}\int \mathrm{Idt} = \frac{1}{C}\int \frac{\mathrm{dQ}}{\mathrm{dt}} \mathrm{dt} = \frac{Q}{C} \quad (12)$$

### 3.3 Piezoelectric Transducer

To describe the electromechanical behavior of the piezoelectric behavior of materials. The first equation generalizes the direct piezoelectric phenomenon whereas the second equation represents the indirect phenomenon of piezoelectric materials.
The collected charge on the surface of the electrode can be expressed as,

$$Q = b\int_0^{L_b} (d_{31} T + \varepsilon_{33} E)\mathrm{dx} \quad (13)$$

Here, $T$ is the mechanical stress, $E$ is electric filed, $d_{31}$piezoelectric constant, and b is constant.

DOI: https://doi.org/10.71058/jodac.v9i1005

Consider the potential difference between the lower and upper electrodes of the piezoelectric layer is denoted as V. The electric field is expressed as,

$$E = -\frac{V}{t_{\text{piezo}}} \tag{14}$$

Here, $t_{\text{piezo}}$ is the piezoelectric layer thickness.
Substitute the value of $E$ in the above equation as follows:

$$Q = \frac{\text{bt}_s d_{31}}{2}[\phi(0) - \phi(L_b)] - \text{bL}_b \varepsilon_{33} \frac{V}{t_{\text{piezo}}} \tag{15}$$

Here, the slope of beam deflection is $\phi$ and, substrate thickness is $t_{\text{piezo}}$.
The magnitude of the current is given as follows:

$$I = \omega\text{Q} = \frac{V}{R} = \frac{\omega \text{bt}_s d_{31}[\phi(0) - \phi(L_b)]}{2\left(1 + \text{bL}_b \varepsilon_{33} \frac{\omega \text{R}}{t_p}\right)} \tag{16}$$

The harvested power of piezoelectric sensors depends upon external loading. The optimal value of loading resistance maximizes the output power [1].
The optimal load resistance in terms of piezoelectric coupling coefficient, $k$ and damping ratio, $\zeta$ and capacitance of piezoelectric sensor, $C_p$ is given as follows:

$$R_{\text{opt}} = \frac{2\zeta}{\omega_n C_p \sqrt{4\zeta + k^4}} \tag{17}$$

Therefore, the optimal power is given as follows:

$$P_{\text{opt}} = \text{I}^2 R_{\text{opt}} = \left(\frac{\omega \text{bt}_s d_{31}[\phi(0) - \phi(L_b)]}{2\left(1 + \text{bL}_b \varepsilon_{33} \frac{\omega \text{R}}{t_p}\right)}\right)^2 R_{\text{opt}} \tag{18}$$

The output voltage of the piezoelectric is given by,

$$V = \frac{\text{Ed}_{33} \varepsilon_{11} A_d}{C} \tag{19}$$

Here, E is Young's modulus in Pascal. $d_{33}$ is the piezoelectric charge coefficient. $\varepsilon_{11}$ is the applied strain. $A_d$ is the area of the electrodes.

### 3.4 Electromagnetic Transducer

The microphone works on the principle of electromagnetic induction.
Write the expression of Faraday's law of electromagnetic induction.

$$e = \text{N} \times \frac{d\phi}{\text{dt}} \tag{20}$$

Here, e is the induced emf (in volts), N is the number of turns in the coil, $\phi$ is the magnetic flux, and t is the time.

### 3.5 Noise Pollution Energy Converter

The NPEC (Noise Pollution Energy Converter) is a combination of the above-discussed electromagnetic transducer and piezoelectric transducer. For noise pollution monitoring the SPL meter is placed at various locations. In integration, the hardware model of the noise pollution energy converter is placed. The main energy converter unit is a combination of an electromagnetic transducer and a piezoelectric transducer.
Loudspeakers are considered as the source of noise pollution. The number of loudspeakers is denoted by n and the distance of the measurement location from the loudspeaker is given by d.
Combine the values of generated voltages from equation (19) and (20) as follows:
The total voltage developed by the energy converter is,

$$V = N \times \frac{d\phi}{\text{dt}} + \frac{Q}{C} = N \times \frac{d\phi}{\text{dt}} + \frac{\text{Ed}_{33} \varepsilon_{11} \text{dA}_d}{C} \tag{21}$$

### 3.6 Helmholtz Resonator

The acoustic or sound resonators are used to enhance the sound pressure to obtain intense excitation of the structure. There are various approaches like Helmholtz resonator, quarter wavelength resonator, and acoustic mathematical

DOI: https://doi.org/10.71058/jodac.v9i1005

approach which is the better among most. The HR locally modifies the pressure distribution in the tube. Transmission, reflection, and attenuation properties of the tube are indeed greatly affected by the presence of HR. So, it has become essential to tune the HR at desired acoustic properties. Since the maximum sound is generated at the resonance frequency the first step is to find the frequency. The resonance frequency is given by,

$$f_H = \frac{c}{2\pi}\sqrt{\frac{A_{\text{neck}}}{V_R L_R}} \tag{22}$$

Where $V_R$ the static volume of the neck is, $L_R$ is the equivalent length of the neck, Aneck is the area of the neck, and c is the speed of sound.
The length is calculated as follows:

$$L_R = L + 0.6 \times R_{\text{neck}} \tag{23}$$

$$A_{\text{neck}} = \frac{V_R}{L_R q} \tag{24}$$

There are two conditions that need to be followed:
1. Any dimension of the resonator should not exceed a quarter of the wavelength of sound frequency.
2. The height of the resonator must be greater than the diameter of the neck of the resonator.

### 3.7 Amplification system

The op-amp RC integrator with a DC gain circuit is used to amplify the generated voltage from the piezo sensor.

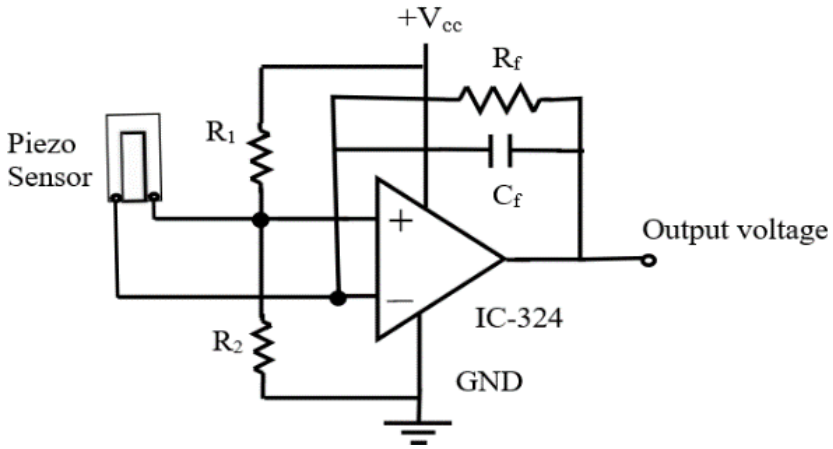


Fig. 3 Op-amp RC integrator with DC gain.

The output voltage of an integrator is given by,

$$v_0 = -\frac{1}{RC}\int v_i dt \tag{25}$$

This also acts as an active low-pass filter. Due to the input voltage divider configuration, the system will be more stable.
DC voltage gain,

$$(Av_0) = 1 + \frac{R_f}{R_1 \| R_2} \tag{26}$$

AC voltage gain,

$$(Av) = \left(1 + \frac{R_f}{R_1 \| R_2}\right) \times \frac{1}{(1+2\pi f C_f R_f)} \tag{27}$$

DOI: https://doi.org/10.71058/jodac.v9i1005

The output voltage is given by,

$$V_o = \left(1 + \frac{R_f}{R_1 \| R_2}\right) \frac{1}{(1+2\pi f C_f R_f)} \left(N \times \frac{d\phi}{dt} + \frac{E d_{33} \varepsilon_{11} dA}{C}\right) \quad (28)$$

Corner frequency,

$$(f_0) = \frac{1}{2\pi C_f R_f} \quad (29)$$

A full wave bridge rectifier is used to convert the AC signal into a DC signal. The DC output voltage of the bridge rectifier is given as follows:

$$V_{DC} = \frac{2V_{in(max)}}{\pi} \quad (30)$$

Here $V_{in(max)}$ is the AC voltage coming from the prior amplification stage.
A capacitive filter is used for filtration of the AC component in the output.
The output power, Pw of the noise pollution energy converter is given as,

$$P_w = 0.0014 \times p^2 \quad (31)$$

## 4. Circuit Development of Noise Pollution Energy Converter

In the initial phase, a noise pollution sensing module was developed on a breadboard using IC-324 (Operational amplifier), LDT0-028K (PVDF film) piezo sensor, analog sound sensor, ESP-8266 Wi-Fi module, jumper wires, and OLED display. External devices such as DSO (Digital signal oscilloscope), multimeter, sound/noise source, and function generator are also used. The implementation of the circuit is shown in Fig. 4.

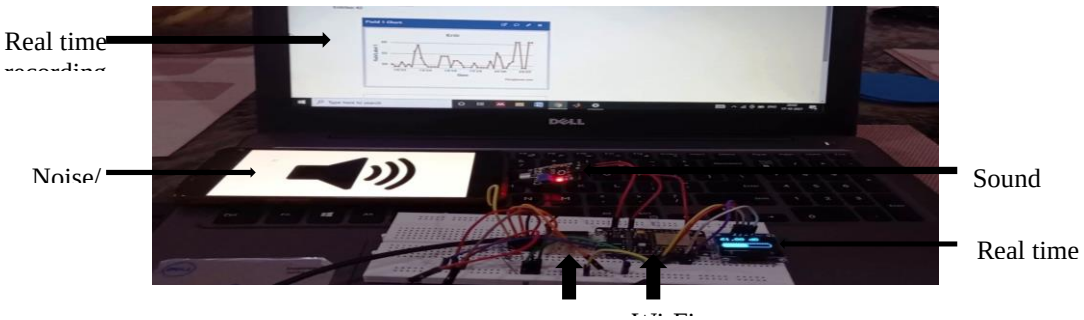


Fig. 4 IOT-based real-time noise monitoring system.

The PVDF film is a piezoelectric transducer that offers a good range of flexibility at low frequencies and high output power density. It is a thin strip of $30 \times 13 \times 1$ mm3 size and negligible weight. This sensor can provide a 7V maximum voltage, 3.2nC electric charge, and 180Hz resonant frequency. Adding the mass to the PVDF film's tip can improve the performance of the film. Later, two PVDF films are connected in parallel and fed to IC-324.

DOI: https://doi.org/10.71058/jodac.v9i1005

TABLE 2: Result of the hardware circuit testing

| S. No. | SPL (dB) | Output Voltage (in volts) | | |
|---|---|---|---|---|
| | | Case-I | Case-II | Case-III |
| 1 | 65 | 0.02 | 0.06 | 0.01 |
| 2 | 67 | 0.03 | 0.13 | 0.03 |
| 3 | 72 | 0.06 | 0.1 | 0.05 |
| 4 | 74 | 0.07 | 0.06 | 0.09 |
| 5 | 77 | 0.07 | 0.1 | 0.13 |
| 6 | 78 | 0.03 | 0.07 | 0.11 |
| 7 | 80 | 0.04 | 0.06 | 0.03 |
| 8 | 82 | 0.08 | 0.12 | 0.05 |
| 9 | 83 | 0.1 | 0.13 | 0.14 |
| 10 | 84 | 0.11 | 0.13 | 0.04 |
| 11 | 85 | 0.12 | 0.18 | 0.34 |
| 12 | 87 | 0.14 | 1.04 | 0.18 |
| 13 | 88 | 0.13 | 0.23 | 0.28 |
| 14 | 89 | 0.14 | 1.07 | 0.17 |
| 15 | 90 | 0.15 | 0.28 | 0.26 |
| 16 | 92 | 0.15 | 0.48 | 0.64 |
| 17 | 93 | 0.14 | 0.32 | 0.89 |
| 18 | 94 | 0.11 | 0.24 | 0.35 |
| 19 | 95 | 0.27 | 0.77 | 0.27 |
| 20 | 101 | 0.41 | 1.72 | 0.39 |

Analog sound sensor is used to detect the sound signal. Fig. 4 shows an IOT based real-time monitoring system for noise pollution. The system comprises ESP-8266, OLED display. Noise produced from vehicular noise was monitored and displayed in terms of SPL on Thing-Speak as well as OLED. Fig. 5 shows the RT (Real-time) noise pollution monitoring as well as energy conversion of noise pollution. The developed system was tested in live circumstances (in daytime & medium traffic condition).

DOI: https://doi.org/10.71058/jodac.v9i1005

Fig. 5 Circuit testing under live circumstances.

The output readings recorded from the set-up are compiled as shown in Figure 6. It is observed that the input and output have linear relation with crisp raise in voltage for slight increment in the SPL for above 40 dB noise level. Up to 50 dB noise level, the voltage ranges from zero to 65 mV. Beyond 50 dB, the voltage boosts up to 200 mV. For 62dB of noise level, the model recorded 206 mV of output voltage. The model shows better performance than a few cited papers [7], [9], and [18].

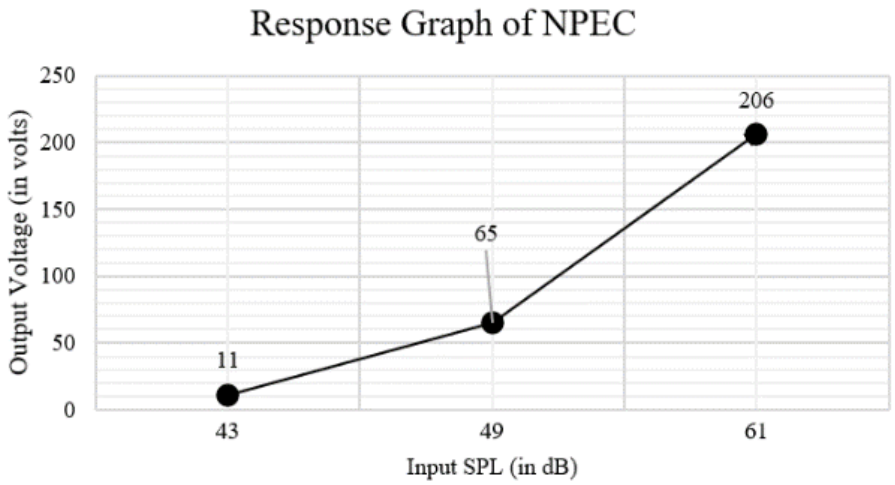


Fig. 6 Response of Noise Pollution Energy Converter.

## 5. Improved Noise Pollution Energy Converter

The improved noise pollution energy converter is only possible via doing the improvement and modification of the circuit. To increase the output voltage, combination of four Piezo sensors (3 parallel and 1 series) are used in series with electromagnetic transducer as shown in Figure 7. The circuit is simplified with reduced wire connections to reduce the losses. The circuit implementation is shown in Figure 8.

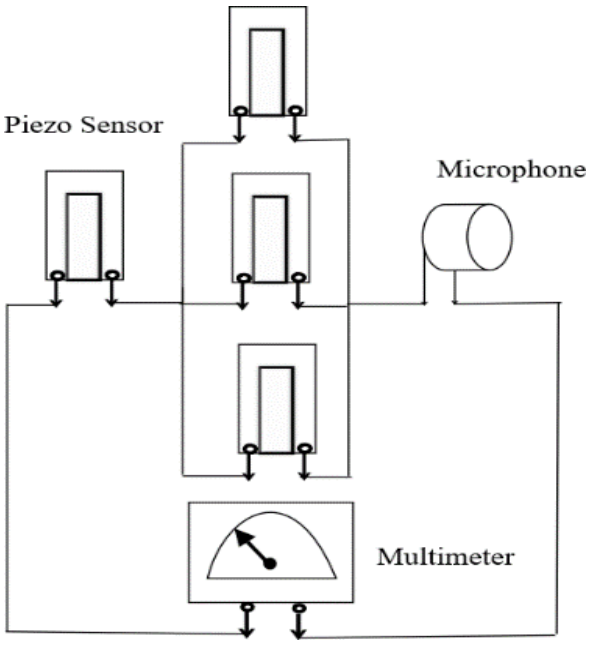


Fig. 7 Circuit connection of modified experimental setup.

DOI: https://doi.org/10.71058/jodac.v9i1005

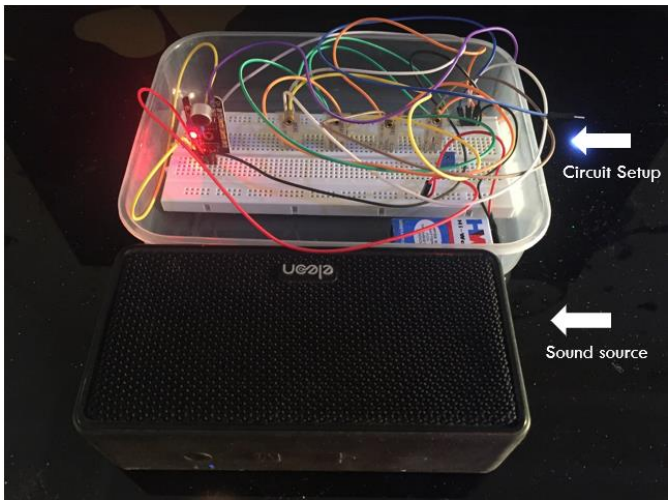


Fig. 8 Hardware setup of modified circuit setup with 3 parallel-1 series connected Piezo sensor.

The hardware setup of improved noise pollution energy converter (NPEC) comprises of Bluetooth speaker as sound/noise source, Sound-meter android application for SPL measurement, 9V DC battery for power the breadboard setup. In breadboard setup, 3 parallel and 1 series combination of piezoelectric sensors with attached proof mass are connected to electromagnetic sound sensor.

An experimental setup is created with the modified circuit shown in Figure 8 placed inside the PET chamber to provide isolation to the NPEC system. The PET (Polyethylene Terephthalate) plastic material based rectangular box of dimension $13.5'' \times 9.5'' \times 7.5''$ is used as a chamber. The chamber neck of 2.2 cm diameter is created at the center of front face of the chamber. The arrangement is shown in Figure 9.

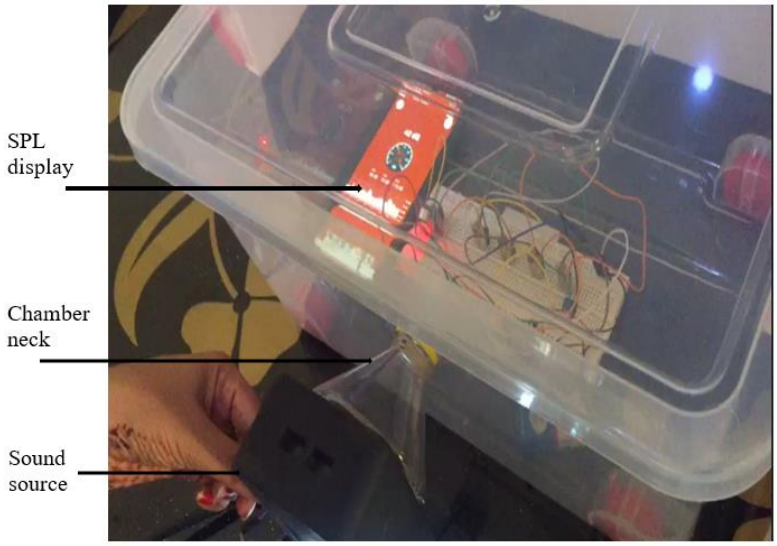


Fig. 9 Experimental setup using PET chamber.

The performance of the NPEC is evaluated with and without the isolation as shown in Figure 11. The circuit is tested for three diverse conditions:

- Case-I: Source outside chamber
- Case-II: Source inside chamber
- Case-III: Without chamber

In case I, the sound source is placed outside the entrance of the chamber through the chamber neck. The chamber acts as a Helmholtz resonator for low input frequency signal. The breadboard circuit and SPL display unit are placed inside the chamber. The multimeter is placed outside for the voltage measurement. In case-II, the chamber entrance is fully closed and provides complete isolation. The sound unit is placed inside the chamber along with the breadboard circuit and SPL display unit. On the other hand, in case-III, the chamber is not used, and the breadboard

DOI: https://doi.org/10.71058/jodac.v9i1005

circuit is tested without chamber. The response graph of the output voltage for the applied sound pressure level is provided in Figure 8. It is observed that the case-II gives the best response and highest peak voltages at various instances. Case-III provides better results compared to Case-I. Case-I gives the lowest output voltages at the same SPL input. The actual data is given in Table 2 and a comparative response graph is shown in Figure 10.

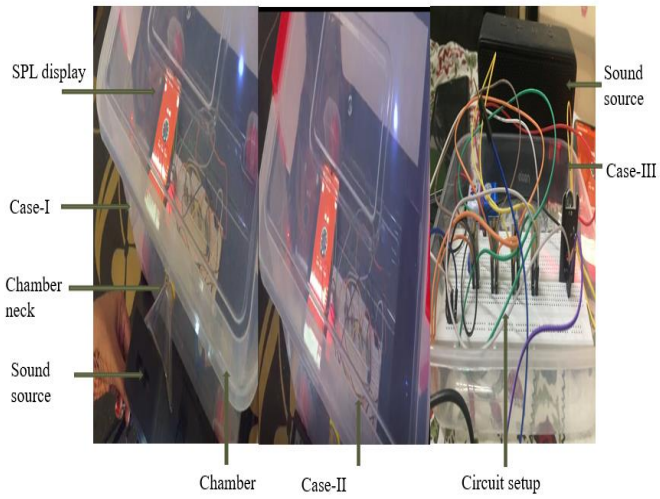


Fig. 10 Hardware circuit testing: Case-I, Case-II, and Case-III (from left to right).

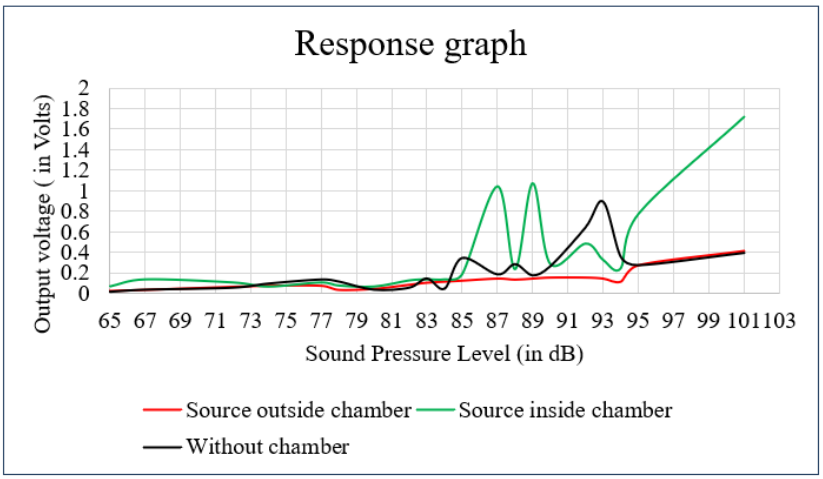


Fig. 11 Comparative graph response of Improved NPEC.

## 6. Improved Amplification Module And Result Analysis

The simulation of the op-amp RC integrator with DC gain circuit shown in Fig. 3 is simulated on NI-Multisim software that provides nearly 104 voltage gain [20]. The waveform contains some offset that can be attenuated using the improved amplification module.

### Improved Amplifier Unit

The amplifier unit has been modified to reduce the offset voltage present in the amplifier unit. The feedback resistance and capacitance values are modified and a step-up transformer with a parallel capacitor is supplied by the output of the integrator. The output waveform of the improved amplifier unit is shown in Figure 12.

DOI: https://doi.org/10.71058/jodac.v9i1005

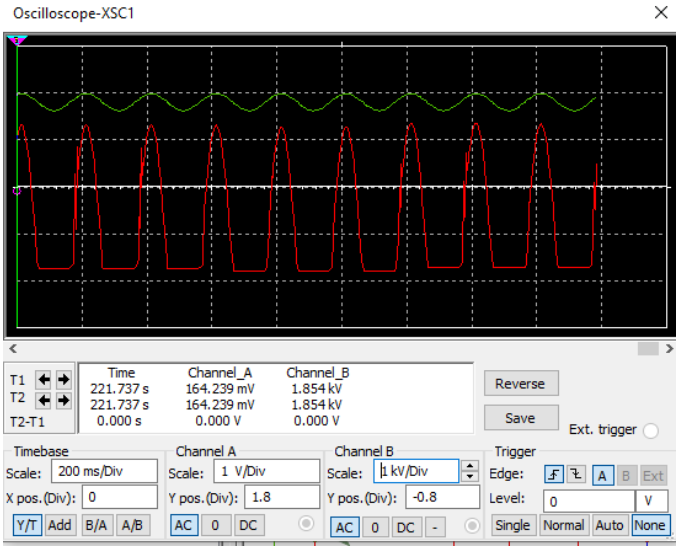


Fig. 12 Output waveform of Improved amplification module.

The improved NPEC without amplification produced 1.04V at 87dB, 1.07V at 89dB, and 1.72V at 101dB SPL respectively. The results are promising and better than the results provided in [12], [14] and [15]. The output waveform of the improved amplification module is much better in comparison to the waveform shown in [20]. The amplification of nearly $2 \times 10^3$ is provided to the input signal. However, the results of software simulation and live experiments might be slightly different but still, the output from the NPEC will get amplified significantly. It is observed that the current and voltage increase proportionally and are in the same phase. It is observed from the experimentation that in the case of constant and continuous input SPL levels, higher electrical energy is obtained in all three cases of improved NPEC.

## 6. Conclusion

The present paper discusses the mathematical modeling and validation for an efficient noise pollution energy conversion system. In this model, the closed chamber is used to confine the sound pressure level to produce the electrical signal and thus it is the advanced oversimplified version of the noise pollution energy converter. This model is validated to show an improved output of the energy conversion in the real-time environment. The modification in the amplification module of NPEC has overcome offset and distortion from the signal. The developed model of noise pollution energy conversion system can be used for various applications such as LED lighting, roadside lighting, traffic signal lights, blind spot displays, powering remotely located CCTV, scientific calculators, etc.

## References

[1] *S. B. Horowitz, M. Sheplak, L. N. Cattafesta, and T. Nishida, "A MEMS acoustic energy harvester", J. Micromechanics Microengineering, vol. 16, no. 9, 2006, doi: 10.1088/0960-1317/16/9/S02.*

[2] *A. Phipps, F Liu, L Cattafesta, M Sheplak, T Nishida. "Demonstration of a wireless, self-powered, electroacoustic liner system", J Acoust Soc Am. 2009 Feb;125(2):873-81. doi: 10.1121/1.3050287.*

[3] *Y. Chen, C. Chang, and T. F. Girls, "Lightning Rabbit – An Application of Sound Energy",APEC youth scientist journal, vol. 3, pp. 161–166, 2010.*

[4] *X. Tang and L. Zuo, "Vibration energy harvesting from random force and motion excitations", Smart Mater. Struct., vol. 21, no. 2, pp. 1–9, 2012, doi: 10.1088/0964-1726/21/7/075025.*

[5] *B. Jo, D. Lee, J. Park, and C. Yeom, "An Experimental Investigation of Noise Energy Generation", ICCECE-2012, Manila, Philippines, 2012, pp. 158–161.*

[6] *B. Li, J. H. You, and Y. J. Kim, "Low frequency acoustic energy harvesting using PZT piezoelectric plates in a straight tube resonator", Smart Mater. Struct., vol. 22, no. 5, 2013, doi: 10.1088/0964-1726/22/5/055013.*

DOI: https://doi.org/10.71058/jodac.v9i1005


[7] G. R. A. Jamal, H. Hassan, A. Das, J. Ferdous, and S. A. Lisa, "Generation of usable electric power from available random sound energy", ICIEV, Dhaka, Bangladesh, 2013, doi: 10.1109/ICIEV.2013.6572549.

[8] H. Y. Lee and B. Choi, "A multilayer PVDF composite cantilever in the Helmholtz resonator for energy harvesting from sound pressure", Smart Mater. Struct., vol. 22, no. 11, 2013, doi: 10.1088/0964-1726/22/11/115025.

[9] F.U. Khan, Izhar. "Hybrid acoustic energy harvesting using combined electromagnetic and piezoelectric conversion", Rev Sci Instrum. 2016, 87(2):025003. doi: 10.1063/1.4941840.

[10] L. H. Fang, S. I. S. Hassan, R. A. Rahim, M. Isa, and B. Bin Ismail, "Charaterization of Differents Dimension Piezoelectric Transducer for Sound Wave Energy Harvesting", Energy Procedia, vol. 105, pp. 836–843, 2017, doi: 10.1016/j.egypro.2017.03.398.

[11] C. S. Salvador et al., "Development of a traffic noise energy harvesting standalone system using piezoelectric transducers and super-capacitor", ICSEng, Las Vegas, USA, pp. 370–376, 2017, doi: 10.1109/ICSEng.2017.77.

[12] M. Yuan, Z. Cao, J. Luo, J. Zhang, and C. Chang, "An efficient low-frequency acoustic energy harvester", Sensors Actuators, A Phys., vol. 264, no. May, pp. 84–89, 2017, doi: 10.1016/j.sna.2017.07.051.

[13] S. Park, Y. Kim, H. Jung, J. Y. Park, N. Lee, and Y. Seo, "Energy harvesting efficiency of piezoelectric polymer film with graphene and metal electrodes", Sci. Rep., vol. 7, no. 1, pp. 1–8, 2017, doi: 10.1038/s41598-017-17791-3.

[14] Y. Wang et al., "A renewable low-frequency acoustic energy harvesting noise barrier for high-speed railways using a Helmholtz resonator and a PVDF film", Appl. Energy, vol. 230, no. July, pp. 52–61, 2018, doi: 10.1016/j.apenergy.2018.08.080.

[15] H. M. Noh, "Acoustic energy harvesting using piezoelectric generator for railway environmental noise", Adv. Mech. Eng., vol. 10, no. 7, pp. 1–9, 2018, doi: 10.1177/1687814018785058.

[16] Y. A. Farghaly, F. A. A. Hemeida, and S. Salah, "Noise utilization as an approach for reducing energy consumption in street lighting", PLoS One, vol. 14, no. 7, pp. 1–20, 2019, doi: 10.1371/journal.pone.0219373.

[17] J. Hossain, N. Sadad Ovi, and M. Monirujjaman Khan, "Design and Investigation of Energy Harvesting System from Noise", Energy Power Eng., vol. 13, no. 08, pp. 307–321, 2021, doi: 10.4236/epe.2021.138021.

[18] C. Song et al., "Multi-frequency sound energy harvesting using Helmholtz resonators with irradiated cross-linked polypropylene ferroelectret films", AIP Adv., vol. 11, no. 11, p. 115002, 2021, doi: 10.1063/5.0060305.

[19] H. Yuan et al., "A High-Performance Coniform Helmholtz Resonator-Based Triboelectric Nanogenerator for Acoustic Energy Harvesting", Nanomaterials (Basel), pp. 1–14, 2021, doi: 10.3390/nano11123431.

[20] A. K. Singh, S. Khatoon, Kriti and P. Ibraheem, "Modeling and Experimental Setup for Noise Pollution Energy Converter", GlobConPT, New Delhi, India, 2022, pp. 1-4, doi: 10.1109/GlobConPT57482.2022.9938.